Biochemistry and Biophysics Reports 34 (2023) 101473

Contents lists available at ScienceDirect

Biochemistry and Biophysics Reports

journal homepage: www.elsevier.com/locate/bbrep

Development of liposomal contrast agent with high iodine concentration and minimal effect on renal function

Tomoko Ochi [a], Hideyuki Nishiofuku [a,*], Tomoko Kure [b], Natsuhiko Saito [a], Ryosuke Taiji [a], Nagaaki Marugami [a], Toshihiro Tanaka [a], Hiromi Sakai [b]

[a] Department of Diagnostic and Interventional Radiology, Nara Medical University, Kashihara, Japan
[b] Department of Chemistry, Nara Medical University, Kashihara, Japan

ARTICLE INFO

Keywords:
Iodinated contrast agent
Liposome
Nephrotoxicity
Contrast-induced acute kidney injury
Liposomal contrast agent

ABSTRACT

Purpose: The use of contrast media is essential to achieve high accuracy in diagnostic imaging. Iodine contrast media, one of these contrast media, has nephrotoxicity as a side effect. Therefore, the development of iodine contrast media that can reduce nephrotoxicity is expected. Since liposomes are generally adjustable in size (100–300 nm) and are not filtered by the renal glomerulus, we hypothesized that iodine contrast media could be encapsulated in liposomes and administered to avoid the nephrotoxicity of iodine contrast media. The aim of this study is to develop an iomeprol-containing liposome (IPL) agent with high iodine concentration and to investigate the effect of intravenous administration of IPL on renal function in a rat model with chronic kidney injury.
Materials and methods: IPLs were prepared by encapsulating an iomeprol (400mgI/mL) solution in liposomes by a kneading method using a rotation–revolution mixer. Radiodensities of iomeprol and IPL were measured. IPL or iopamidol at normal dose (0.74 g I/kg) or high dose (3.7 g I/kg) was administered to healthy and 5/6-nephrectomized rats (n = 3–6). Serum creatinine (sCr) and histopathological change of tubular epithelial cells were evaluated after injection.
Results: The iodine concentration of IPL was 220.7 mgI/mL, equivalent to 55.2% of the iodine concentration of iomeprol. The CT values of IPL was 4731.6 ± 53.2 HU, 59.04% that of iomeprol. The ratios of change in sCr in 5/6-nephrectomized rats that received high-dose iopamidol were 0.73, which were significantly higher than that in 5/6-nephrectomized rats that received high-dose IPL (−0.03) ($p = 0.006$). Change in foamy degeneration of tubular epithelial cells was confirmed in 5/6-nephrectomized rats that received high-dose iopamidol than that in the sham control group and healthy rats that received normal dose iopamiron ($p = 0.016$, $p = 0.032$, respectively). Foamy degeneration of tubular epitherial cells was rarely observed in the IPL injection group.
Conclusions: We developed new liposomal contrast agents that have high iodine concentration and minimal effect on renal function.

1. Introduction

Medical diagnostic imaging visualizes life phenomena in a minimally invasive manner [1,2] and plays a major role in diagnosing pathological conditions, determining treatment strategies and effects, and predicting prognosis. Recent developments in therapeutic techniques require precise imaging findings, and the importance and demand for tests using contrast media is increasing [3,4]. However, iodinated contrast agents can cause contrast-induced acute kidney injury (CI-AKI), a severe adverse event that accounts for one-third of hospital-acquired acute kidney injury. Patients with CI-AKI have a higher risk of in-hospital adverse events, prolonged hospital stay, and long-term mortality compared with those without CI-AKI. Chronic kidney disease (CKD) is considered the most important risk factor for CI-AKI in humans [5]. According to several epidemiologic studies, the prevalence of CKD is 10.8%–16.8% in the general population and shows an increasing trend [5]. Therefore, the development of contrast agents that have minimal effect on renal function is essential.

Liposomes are spherical vesicles composed of a lipid bilayer envelope surrounding a central aqueous core. Various contrast and treatment agents have been encapsulated in liposomes for diagnostics, therapy, and preventive medicine [6–8]. After administration into the blood

* Corresponding author. Shijocho 840, Kashihara, Nara, Japan.
E-mail address: hnishiofuku@gmail.com (H. Nishiofuku).

https://doi.org/10.1016/j.bbrep.2023.101473
Received 19 January 2023; Received in revised form 12 April 2023; Accepted 17 April 2023

circulation, liposomes are gradually entrapped by the mononuclear phagocyte system, by such as Kupffer cells in the liver and macrophages in the spleen, and subsequently excreted into feces within a few weeks [9,10]. It has been reported that liposomal iodinated contrast agents do not exhibit significant renal clearance [11]. We hypothesized that liposomal iodinated contrast agents have different pharmacokinetics and minimal effect on renal function compared with free iodinated contrast agents.

It is difficult to encapsulate iodinated contrast agents using the conventional liposome preparation method because of their high viscosity at the required concentration [12]. Therefore, we attempted to prepare liposomes by encapsulating a solution of iodinated contrast agent, applying a kneading method using a rotation-revolution mixer, developed previously for preparing liposome-based artificial red blood cells [13]. The kneading method using a rotation-revolution mixer, takes advantage of the high viscosity of the liposomes and uses shear stress to encapsulate a thick, viscous liquid into liposomes [14]. Circulation stability and dispersion stability of liposomal artificial red blood cells prepared by this technique has been reported previously [10,14].

The aims of this study were to prepare an iomeprol-containing liposome (IPL) agent and to determine its effect on renal function following intravenous administration in a rat model with chronic kidney injury.

2. Materials and methods

2.1. Preparation of liposome agent

We prepared IPL by the kneading method using a rotation−revolution mixer [14]. We purchased 1,2-dipalmitoyl-sn-glycero-3-phosphatidylcholine (DPPC) from H. Holstein Co., Ltd. (Tokyo, Japan), and purchased cholesterol and 1,5-Odihexadecyl- N-succinyl-L-glutamate (DHSG) from Nippon Fine Chemical Co., Ltd. (Osaka, Japan). 1,2-Distearoyl-snglycero- 3-phosphatidylethanolamine-N-poly (ethylene glycol) (PEG5000, PEG−DSPE) was purchased from NOF Corp. (Tokyo, Japan). Selected lipids at specific molar ratios (DPPC/cholesterol/DHSG/PEG-DSPE = 5/4/0.9/0.03) were dissolved in 2-methyl-2-propanol (500 mL; Fujifilm Wako Pure Chemical Corp., Osaka, Japan) by stirring in a 500 mL flask at 60 °C. The lipid mixture solution was then freeze-dried (EYELA FD-1000; Tokyo Rikakikai Co., Ltd., Tokyo, Japan) for 1 day to obtain a powdered lipid mixture.

Iomeprol (80 mL, 400 mgI/mL; Iomeron, Bracco Imaging Eisai, Tokyo, Japan) and mixed lipid powder (20 g) were placed in a cylindrical polytetrafluoroethylene container (outer diameter, 93 mm; height, 110 mm; with multiple concave inner surfaces) and kneaded using a rotation−revolution mixer (ARE-500; Thinky Corp., Tokyo, Japan) at 1000 rpm for clockwise revolution and at 1000 rpm for counterclockwise rotation, for 5–30 min. The obtained iomeprol−lipid mixture paste was dispersed with saline (Otsuka Pharmaceutical Co., Ltd., Tokyo, Japan) and then filtered through 0.80 μm filters (Advantec cellulose acetate hydrophilic filter; Toyo Roshi Kaisha Ltd., Tokyo, Japan). After separating unencapsulated iomeprol by ultracentrifugation (Himac CP80WX; Hitachi Ltd., Tokyo, Japan) at 19,000 rpm for 60 min, the precipitate was re-dispersed with saline and the dispersion was filtered through 0.80 μm filters.

Aseptic conditions were ensured by making all raw materials sterile and preparing them in a clean room.

2.2. Characterization of liposomes

Particle size was measured using a dynamic light-scattering method (nanoparticle analyzer, SZ-100; Honda Ltd., Kyoto, Japan) according to existing methods [13]. The total lipid concentration of reluctant liposomes was estimated from the phospholipid concentration measured using the choline oxidase-DAOS method [Wako Pure Chemical Corp. Ltd.; DAOS: N-ethyl-N-(2-hydroxy3-sulfopropyl)-3,5-dimethoxyaniline]. To measure the concentration of iomeprol in IPL solution, octylglucoside was added to completely dissolve the liposomes. Iomeprol has a characteristic absorption in the UV region at $\lambda_{max} = 244$ nm. A calibration curve was prepared by changing the concentration of iomeprol, and the concentration was determined based on this curve.

2.3. Assessment of CT absorption of IPL

CT images of iomeprol (400 mgI/mL), iopamidol (300 mgI/mL; Iopamiron 300, Bayer, Osaka, Japan) and IPL (220.7 mgI/mL) were obtained using a cylindrical water-filled phantom. Three test tubes (inner diameter, 8 mm) filled with each of iomeprol (400 mgI/mL), iopamidol (300 mgI/mL), and IPL were placed in the phantom and scanned by a 320 area detector CT scanner (Aquilion ONE, Canon Medical Systems, Japan) at applied voltage of each of 100 kVp and 120 kVp. The imaging conditions were as follows: tube current, 50 mA; rotation time, 1.0 s; pitch factor, 0.813; and 80 × 0.5 mm detectors. The obtained filtered back-projection images were reconstructed with a display field of view of 100 mm, nominal slice thickness of 5 mm, and abdominal standard reconstruction kernel FC13. CT attenuation values were measured and compared among the iodinated solutions.

2.4. Animals

All animals were purchased from CLEA Japan Inc., Tokyo, Japan. Healthy male Sprague–Dawley rats and those that had undergone 5/6 nephrectomy (300–380g, 15 weeks old) were used in this study. The animals were housed in groups of two per cage in a temperature-controlled room on a 12-h light/dark cycle. They were allowed free access to food and water. All experimental protocols were reviewed by the Committee on the Ethics of Animal Experiments at our university and conducted in accordance with the Guidelines for Animal Experiments issued by our university and with law No. 105 (Act on Welfare and Management of Animals) issued by the Japanese government. The ethical guidelines conformed to the guiding principles issued by the National Academy of Science.

2.5. Experimental protocol

The experimental protocol is shown in Fig. 1. First, either contrast agent or normal saline was injected intravenously slowly over 1 min via the tail vein after oral administration of normal saline for one week. Second, additional intravenous injection of the same dose of contrast agent or normal saline slowly over 1 min was performed after dehydration for 48 h. Third, rats were dehydrated for 24 h after the second injection, and then sacrificed by intravenous administration of 60 mL/kg pentobarbital. The kidneys were harvested for histopathological evaluation [5,15].

The rats were divided into seven groups and different drugs and dosages were administered in each group as follows (Table 1): (1) sham control group (n = 5): 40 mL/kg normal saline; (2) RN group, n = 6: normal-dose (2 mL/kg) iopamidol (370 mgI/mL; Iopamiron 370, Bayer, Osaka, Japan) and 38 mL/kg normal saline simultaneously; (3) RH group, n = 6: high-dose (10 mL/kg) Iopamidol (370 mgI/mL) and 30 mL/kg normal saline simultaneously; (4) NxN) group (n = 3): 5/6 (83%) nephrectomized rats injected with normal-dose (2 mL/kg) Iopamidol (370 mgI/mL) and 38 mL/kg normal saline simultaneously; (5) NxH group (n = 6): 5/6 nephrectomized rats injected with high-dose (10 mL/kg) Iopamidol (370 mgI/mL) and 30 mL/kg normal saline simultaneously; (6) NxNL group (n = 3): 5/6 nephrectomized rats injected simultaneously with normal-dose IPL (0.74 gI/kg) and normal saline simultaneously, to achieve a total of 40 mL/kg body weight per administration; (7) NxHL group (n = 5): 5/6 nephrectomized rats injected simultaneously with high-dose IPL (3.7 gI/kg) and normal saline simultaneously, to achieve a total of 40 mL/kg body weight per administration. The iodine concentration of IPL was measured by the

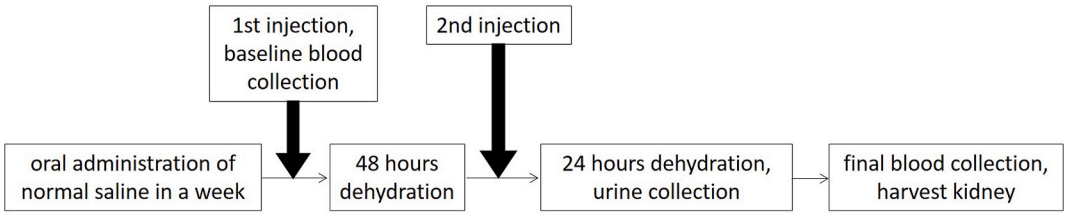

Fig. 1. Experimental protocol.

Table 1
The name of groups and characteristics of groups.

Name of groups	characteristics of groups
CR	control rats
RN	healthy rats + normal dose iopamiron
RH	healthy rats + high dose iopamiron
NxN	5/6 nephrectomy rats + normal dose iopamiron
NxH	5/6 nephrectomy rats + high dose iopamiron
NxNL	5/6 nephrectomy + normal dose IPL
NxHL	5/6 nephrectomy + high dose IPL

The name of groups and characteristics of groups are shown.

method described above, and the dose was determined.

2.6. Biological samples

Baseline blood samples (1.5 mL) were collected from the tail vein before the first injection, and again after dehydration for 24 h following the second injection. Serum was then separated from whole blood. Each sample was centrifuged (3000 rpm for 10 min at 4 °C), and the plasma was immediately frozen using liquid nitrogen and stored at −80 °C. After the second injection, all rats were transferred to individual metabolic cages and urine samples were collected for 24 h from each rat separately. Because of their small size, liposomes remain in the serum after centrifugation and interfere with clinical laboratory tests [16]. To precipitate the liposomes by conventional centrifugal separation of blood, Dextran (Mw. 450–650 kDa; final concentration: 2.6 g/dL in blood) was added to the blood and urine samples of the NxNL and NxHL groups [17].

Serum creatinine (sCr), blood urea nitrogen (BUN), serum albumin, and urinary protein concentrations were measured using an automatic biochemistry analyzer at Sanritsu Zelkova Laboratory. The ratios of changes in sCr, BUN, and serum albumin before and after the injection of contrast agent or normal saline were calculated as follows.

$$ratio\ of\ change = \frac{V2 - V1}{V1}$$

In that equation, V1 and V2, respectively, denote biochemical test value from the baseline blood collection and the final blood collection.

2.7. Histopathological examination of kidney tissue

Kidney tissue was fixed in 10% buffered formalin for 24 h and then dehydrated in a graded series of ethyl alcohol. For histologic examination, the tissue was cut into 3-mm-thick slices and paraffinized; 2-μm-thick slices were then deparaffinized and stained with hematoxylin and eosin. For semiquantitative analysis of the frequency and severity of renal lesions, we randomly selected three high-magnification (× 200) fields of the cortex and outer stripe of the outer medulla. Foamy degeneration was graded as follows: 0 = no damage, 1 = mild (<25% damage), 2 = moderate (25%–50% damage), 3 = severe (50%–75% damage), or 4 = very severe (>75% damage) [5].

2.8. Statistical analysis

Statistical analysis was performed using the statistical software IBM SPSS Statistics 25. All data are presented as the mean ± SD. One-way analysis of variance (ANOVA) was used to compare means among groups. Upon detection of significant differences by ANOVA, post-hoc pairwise comparisons were conducted using Tukey's test, with the level of statistical significance taken as $P < 0.05$.

3. Results

3.1. Characterization and CT attenuation values of IPL

The physiochemical parameters of IPLs were as follows: particle diameter, 283.6 ± 3.8 nm; iodine concentration, 213.6 ± 3.7 mgI/mL; concentration of lipids, 8.0 ± 0.1 g/dL; poly-dispersity index, 0.054 ± 0.006; encapsulation efficiency, 17.5 ± 0.7%. The results of the latest five preparations (Table 2) indicate that IPL could be prepared stably. The iodine concentration ratio of IPL was 54.7% that of iomeprol. Fig. 2 shows a CT image of the three contrast media in the phantom. The CT attenuation values of iomeprol (400 mgI/mL), iopamidol (300 mgI/mL), and IPL (220.7 mgI/mL) at 120 kVp were 8013.8 ± 140.8, 6273.6 ± 110.2, and 4731.6 ± 53.2 Hounsfield units (HU), respectively. The ratio of the CT attenuation values of IPL and iomeprol was 59.0%. At 100 kVp, the CT attenuation values of iomeprol and IPL were 10,358.4 ± 138.8 and 5995.4 ± 47.3 HU, respectively. The CT attenuation value of IPL at 100 kVp was close to that of iopamidol (300 mgI/mL) at 120 kVp (5995.4 ± 47.3 HU vs. 6273.6 ± 110.2).

3.2. Biochemical evaluation

Fig. 3 shows the ratios of change in sCr, BUN, serum albumin before and after the injection of contrast agent or normal saline, and urinary protein concentrations. In the normal rats, the pre and post sCr values in the sham control group were 0.31 ± 0.01 and 0.37 ± 0.02 mg/dL, respectively, and the ratio of change was 0.18. The ratio of change in the RN group was 0.17 (pre, 0.60 ± 0.01 mg/dL; post, 0.70 ± 0.02 mg/dL), and that in the RH group was 0.43 (pre, 0.27 ± 0.01 mg/dL; post, 0.38 ± 0.02 mg/dL). In the RH group, sCr increased by more than 25% compared to pre-treatment. There was no significant difference between the sham control and RN groups ($P = 1.000$), the sham control and RH groups ($P = 0.783$). In the groups of 5/6-nephrectomized rats that received iodinated contrast agents, the ratio of change in the NxN group

Table 2
Physiochemical parameters of IPL.

Lot number	Particle diameter (nm)	Iodine concentration (mg/mL)	Concentration of lipids (g/dL)
1	301.3	212.0	7.99
2	277.0	219.3	8.04
3	271.5	229.5	7.44
4	302.1	220.7	8.63
5	310.2	232.6	8.19

Results are shown for the latest five preparations of IPL.
IPL: iomeprol-containing liposome.

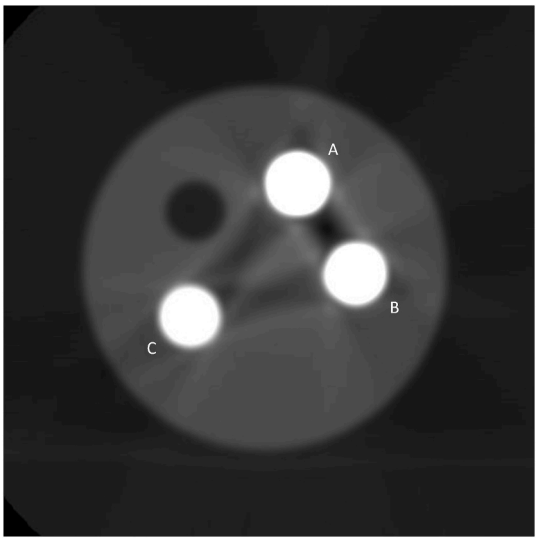

Fig. 2. CT phantom image obtained at 120 kV showing the various agents. Test tubes (inner diameter, 8 mm) filled with A: iomeprol (400 mgI/mL), B: Iopamiron (300 mgI/mL), C: IPL (220.7 mgI/mL) were placed within a cylindrical water-filled phantom. The CT values of iomeprol, Iopamiron, and IPL at 120 kVp were 8013.77 ± 140.84, 6273.55 ± 110.26, and 4731.62 ± 53.24 Hounsfield units, respectively.
CT: computed tomography, IPL: iomeprol-containing liposome.

was 0.14 (sCr value: pre, 0.55 ± 0.06 mg/dL: post, 0.62 ± 0.08 mg/dL) and that in the NxH group was 0.73 (sCr value: pre, 0.47 ± 0.02 mg/dL; post, 0.83 ± 0.17 mg/dL). In the NxH group, sCr increased by more than 25% compared to pre-treatment. There was no significant difference between the sham control and NxN groups (P = 1.000), the sham control and RH groups (P = 0.078). In the groups of 5/6-nephrectomized rats that received IPL, the ratio of change in the NxNL group was 0.07 (sCr value: pre, 0.53 ± 0.05 mg/dL, post, 0.57 ± 0.08 mg/dL) and that in the NxHL group was −0.03 (sCr value: pre, 0.47 ± 0.03 mg/dL; post, 0.45 ± 0.04 mg/dL). The ratio of change was significantly lower in the NxHL group than in the NxH group (p = 0.006).

The ratio of change in BUN in the sham control group was 0.07 ± 0.07 (pre, 17.08 ± 0.73 mg/dL; post, 18.20 ± 0.86 mg/dL). The ratios of change in serum BUN in the normal rat groups of RN and RH were −0.02 ± 0.05 (pre, 18.63 ± 0.68 mg/dL; post, 18.25 ± 0.87 mg/dL) and 0.23 ± 0.08 (pre, 15.28 ± 0.51 mg/dL; post, 18.65 ± 0.95 mg/dL), respectively. There was no significant difference in the ratio of either of these groups compared with the sham control group (p = 0.999 and p = 0.978, respectively). The ratios of change in serum BUN in the 5/6-nephrectomized rat groups of NxN, NxH, NxNL, and NxHL were −0.20 ± 0.06 (pre, 48.10 ± 7.90 mg/dL; post, 38.40 ± 7.23 mg/dL), 0.21 ± 0.26 (pre, 29.12 ± 1.65 mg/dL; post, 35.86 ± 9.09 mg/dL), −0.14 ± 0.10 (pre, 37.60 ± 4.41 mg/dL; post, 33.10 ± 7.80 mg/dL), and 0.12 ± 0.19 (pre, 30.12 ± 3.31 mg/dL; post, 33.10 ± 5.23 mg/dL), respectively. There was no significant difference in the ratios of the NxN, NxH, NxNL, and NxHL groups compared with the sham control group (p = 0.892, p = 0.989, p = 0.962, and p = 1.000, respectively).

In the normal rats, the pre and post serum albumin values in the sham control group were 4.18 ± 0.10 mg/dL and 4.20 ± 0.06 mg/dL, respectively, and the ratio of change was 0.01 ± 0.02. The ratio of change in serum albumin in the RN group was 0.01 ± 0.00 (pre, 4.38 ± 0.06 mg/dL, post, 4.42 ± 0.06 mg/dL) and that in the RH group was 0.06 ± 0.02 (pre, 4.17 ± 0.07 mg/dL; post, 4.43 ± 0.08 mg/dL). In the groups of 5/6-nephrectomized rats that received iodinated contrast agents, the ratio of change in serum albumin in the NxN group was 0.03

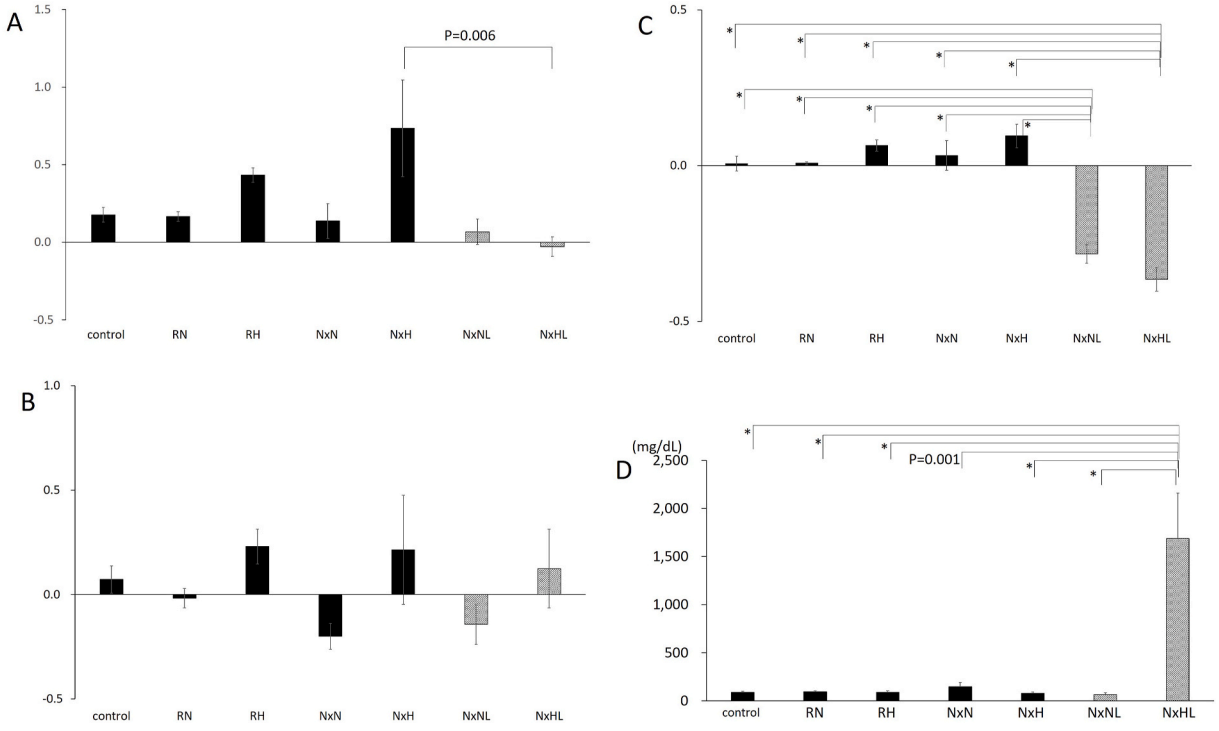

Fig. 3. Change of serum creatinine.
A, Ratio of change of sCr. B, Ratio of change of BUN. C, Ratio of change of serum albumin. D, urinary protein. Data are presented as the mean ± standard deviation (SD). The ratios of change in sCr level were significantly higher in the RH and NxH groups compared with the sham control group. There was no significant difference in sCr between the NxHL and sham control groups. Urinary protein was highest in the NxHL group and was significantly higher in the NxHL group compared with the sham control group. sCr: serum creatinine, BUN: blood urea nitrogen, RN: healthy rats with normal-dose iopamiron, RH: healthy rats with high-dose iopamiron, NxN: 5/6 nephrectomized rats with normal-dose iopamiron, NxH: 5/6 nephrectomized rats with high-dose iopamiron, NxNL: 5/6 nephrectomized rats with normal-dose IPL, NxHL: 5/6 nephrectomized rats with high-dose IPL.

± 0.05 (pre, 4.17 ± 0.09 mg/dL; post, 4.30 ± 0.20 mg/dL) and that in the NxH group was 0.10 ± 0.04 (pre, 3.92 ± 0.10 mg/dL; post, 4.28 ± 0.05 mg/dL). There was no significant difference in ratio of change of serum albumin for any of these four groups compared with the sham control group ($p = 1.000$, $p = 0.691$, $p = 0.998$, and $p = 0.251$, respectively). In the groups of 5/6-nephrectomized rats that received IPL, the ratio of change in serum albumin in the NxNL group was −0.28 ± 0.03 (pre, 4.20 ± 0.17 mg/dL; post, 3.00 ± 0.00 mg/dL) and that in the NxHL group was −0.37 ± 0.04 (pre, 3.82 ± 0.07 mg/dL; post, 2.42 ± 0.12 mg/dL). The ratios of change of serum albumin were significantly lower in the NxNL and NxHL groups than that in the sham control group ($p = 0.000$ and $p = 0.000$, respectively).

Urinary protein concentration was 88.2 ± 12.2 mg/dL in the sham control group. In the normal rats, concentration was 96.3 ± 9.4 mg/dL and 88.8 ± 15.6 mg/dL in the RN and RH groups, respectively, which were not significantly different compared with the sham control group ($p = 1.000$ and $p = 1.000$, respectively). Urinary protein concentrations in the 5/6-nephrectomized rat groups of NxN, NxH, NxNL, and NxHL were 145.3 ± 45.9, 75.6 ± 6.7, 64.0 ± 20.8, and 1686.0 ± 473.3 mg/dL, respectively. There was no significant difference in concentration in the NxN, NxH, and NxNL groups compared with the sham control group ($p = 1.000$, $p = 1.000$, and $p = 1.000$ respectively). Concentration was significantly higher in the NxHL group than in the sham control group ($p = 0.000$).

3.3. Histopathological examination of kidney tissue

Table 3 lists the results of foamy degeneration score in kidney tissues. Representative pathological images in the NxH and NxHL groups are shown in Fig. 4. In the normal rats, scores in the sham control group, RN group, and RH group were 1.8 ± 0.17, 1.0 ± 0.13, and 2.7 ± 0.13, respectively. There was no significant difference between the sham control group and the RN group and RH group ($p = 0.999$, $p = 0.118$, respectively). In the groups of 5/6-nephrectomized rats, foamy degeneration scores in the NxN, NxH, NxNL, and NxHL groups were 1.9 ± 0.44, 3.0 ± 0.24, 2.0 ± 0.19, and 2.2 ± 0.34, respectively. The score was significantly higher than in the sham control group and RN group only in the NxH group ($p = 0.016$, $p = 0.032$, respectively). There was no significant difference in score between the NxHL and sham control groups and RN group.

4. Discussion

Most previous studies of liposomal contrast agents have reported their application to imaging of the liver and spleen, micro vessels, blood pool imaging, and image-guided drug delivery [6,18–22]. To the best of our knowledge, none has evaluated the nephrotoxicity of liposomal iodinated contrast agents.

Our method of liposome preparation uses a rotation–revolution mixer, which enables efficient encapsulation of a highly viscous solution and control of particle size. Using this technique [14], we successfully prepared a large amount of liposome-encapsulating iodinated contrast agent at a higher iodine concentration (220.7 ± 9.3 mgI/mL) than has been reported previously (26.5–120 mgI/mL) [12,18,22–25]. Relative to iomeprol 400, IPL achieved similar rates of iodine concentration and CT attenuation values of 55.2% and 59.0%, respectively. In addition, the CT attenuation value of IPL at 100 kVp was close to that of iopamidol (300 mgI/mL) at 120 kVp. A recent study reported that in dual energy CT with monoenergetic reconstructions at lower energy levels, adequate image quality could be obtained using a 50% reduction in the volume of iodinated contrast medium administered [26]. The results of the present study suggest that IPL might also deliver image quality of sufficient quality for application in the clinical setting. Improvements in imaging of the liver and spleen, micro vessels, blood pool imaging, and image-guided drug delivery, which have been reported previously, are also expected with the use of IPL with high iodine concentration.

A single injection of iodinated contrast agent does not cause overt kidney damage in rats, and an additional insult to the kidney is required to establish clinically manifest CI-AKI [27]. Renal concentrating ability is higher in rats than in humans and may be the factor responsible for resistance to CI-AKI in rats. In the present study, we succeeded in increasing the serum creatinine level in the NxH group by more than 25% compared to the pre-treatment level by the combination of 5/6 nephrectomy, salt loading with oral saline, combined 72-h dehydration, and multiple large doses of iodinated contrast agents. Using this model, large amounts of iodinated contrast agents must be administered. Following the successful preparation of IPL, we administered IPL as a high-dose iodinated contrast agent and evaluated its nephrotoxicity. Nephrotoxicity was apparent in the NxH group, which were injected with high-dose iodinated contrast agents; however, no nephrotoxicity or histopathological damages were observed following the administration of IPL, even in the high-dose group (NxHL). The pathogenesis of CI-AKI is controversial, and two mechanisms have been postulated: renal artery constriction resulting from iodinated contrast agents and subsequent renal hypoperfusion, and tubular damage. Several theories have been proposed for the cause of tubular damage, including direct toxicity, high viscosity, and reactive oxygen species-mediated cellular injury [28,29]. The degree of tubular epithelial cell vacuolization, which is the characteristic histopathological change in CI-AKI, was lower in the IPL group than in the iopamidol group of the present study. Our histopathological results showed that injection of IPL had little effect on the kidney. According to previous reports, liposomes are taken up mainly by the phagocytic cells of the mononuclear phagocytic system following intravenous injection of iodinated liposomes [30]. The liposomal envelope shields the body from the contrast agent, resulting in elimination via the liver and spleen rather than excretion via the kidneys [23].

Serum albumin was significantly lower in the NxNL and NxHL groups than in the other groups. In the present study design, there was a large amount of fluid infusion per body weight of the rats. As liposomes remain in the circulating blood for a long time, we consider that the condition of prolonged excessive fluid volume may have caused this dilution of serum albumin in the NxNL and NxHL groups [31]. In the NxN group a slight decrease in BUN between before and after injection of contrast medium was of limited significance. Urinary protein was significantly higher in the NxHL group than in the other groups. Liposomes are present in the circulating blood for long periods when a high volume is administered. It is known that physiological changes in pregnancy result in increased cardiac output and renal blood flow, with a subsequent increase in proteinuria [32]. One possible reason for the increase in urinary protein in the present study is the increase in renal blood flow due to increased circulating blood volume.

Table 3
Histopathological score of kidney tissue.

Group	dose	Healthy rats	5/6 nephrectomy rats
iopamiron	normal	1.9 ± 0.13	1.9 ± 0.44
	high	2.7 ± 0.13	3.0 ± 0.24*
IPL	Normal	–	2.0 ± 0.19
	high	–	2.2 ± 0.34
Control		1.8 ± 0.17	–

*: $p < 0.05$.
Data are presented as the mean ± standard deviation (SD). The histopathological score of kidney tissue was significantly higher in the NxH groups compared with the sham control group and RN group ($p = 0.016$, $p = 0.032$, respectively). There was no significant difference in score between the NxHL and sham control groups or RN group.
IPL: iomeprol-containing liposome, RN: healthy rats with normal-dose iopamiron, RH: healthy rats with high-dose iopamiron, NxN: 5/6 nephrectomized rats with normal-dose iopamiron, NxH: 5/6 nephrectomized rats with high-dose iopamiron, NxNL: 5/6 nephrectomized with normal-dose IPL, NxHL: 5/6 nephrectomized with high-dose IPL.

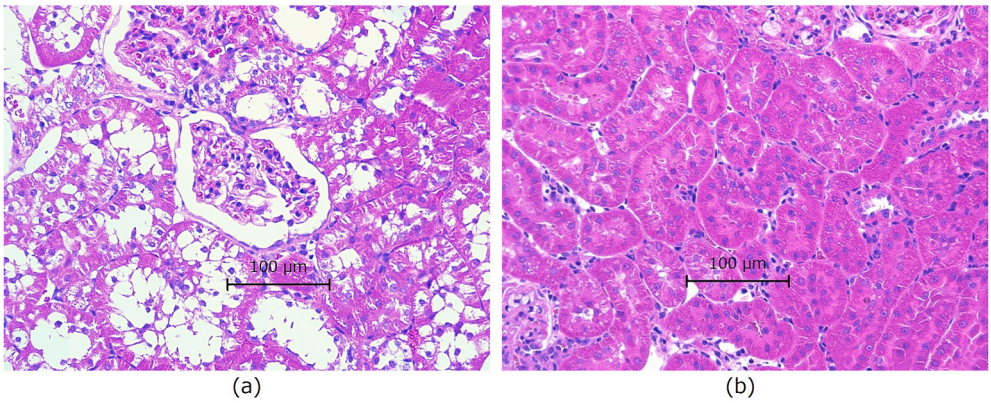

Fig. 4. Histological images of kidney tissue (hematoxylin–eosin staining).
(a) NxH group: injury is apparent as vacuolation of tubular cells, (b) NxHL group: the extent of tubular injury is less than that in the NxH group. NxH: 5/6 nephrectomized rats with high-dose iopamiron, NxHL: 5/6 nephrectomized rats with high-dose IPL.

There were some limitations in this study. The mechanisms of the metabolism and excretion pathways of IPL were not investigated. However, Sakai et al. has reported that similar liposomes to those used in the present study were removed by entrapment by Kupffer cells and by macrophages in the spleen [33]. Finally, we did not examine whether the rats used in our study were an appropriate model for renal failure.

In conclusion, we have developed a new liposomal contrast agent that has a high iodine concentration and minimal effect on renal function. This agent may offer a clinical advantage of reduced renal toxicity compared with conventional iodinated contrast agents and better enhancement and image quality compared to previous liposomal contrast agents.

Conflicts of interest and source of funding

The authors have no Conflicts of interest. This work was supported by JSPS KAKENHI Grant Number JP 21K07323, 19K16956, 17K16475.

Data availability

The data that has been used is confidential.

Acknowledgement

This work was supported by JSPS KAKENHI Grant Number JP 21K07323, 19K16956, 17K16475.

References

[1] Yongxiang Zhu, Baomei Shen, Xuan Pei, Haixia Liu, Li CT. Guoyan, MRI, and PET imaging features in cervical cancer staging and lymph node metastasis, Am J Transl Res 13 (9) (2021) 10536–10544, eCollection 2021.

[2] Angela Giardino, Supriya Gupta, Emmi Olson, Karla Sepulveda, Lenchik Leon, Ivanidze Jana, Rebecca Rakow-Penner, Midhir J. Patel, Rathan M. Subramania, Dhakshinamoorthy Ganeshan, Role of imaging in the era of precision medicine, Acad. Radiol. 24 (5) (2017 May) 639–649, https://doi.org/10.1016/j.acra.2016.11.021.

[3] Ryosuke Taiji, Hideyuki Nishiofuku, Toshihiro Tanaka, Kiyoyuki Minamiguchi, Yasushi Fukuoka, Natsuhiko Saito, Hidehiko Taguchi, Takeshi Matsumoto, Nagaaki Marugami, Toshiko Hira, Kimihiko Kichikawa, Useful parameters in dynamic contrast-enhanced ultrasonography for identifying early response to chemotherapy in a rat liver tumor model, J Clin Imaging Sci 15 (11) (2021) 15, https://doi.org/10.25259/JCIS_6_2020.eCollection2021.

[4] Tomoko Ochi, Toshiaki Taoka, Ryosuke Matsuda, Masahiko Sakamoto, Toshiaki Akashi, Tetsuro Tamamoto, Tadashi Sugimoto, Hiroshi Sakaguchi, Masatoshi Hasegawa, Hiroyuki Nakase, Kimihiko kichikawa, Comparison between two separate injections and a single injection of double-dose contrast medium for contrast-enhanced MR imaging of metastatic brain tumors, Magn. Reson. Med. Sci. 13 (4) (2014) 221–229, https://doi.org/10.2463/mrms.2013-0068. Epub 2014 Aug 27.

[5] Tong-qiang Liu, Wei-li Luo, Xiao Tan, Yi Fang, Jing Chen, Hui Zhang, Xiao-fang Yu, Jie-ru Cai, Xiao-qiang Ding, A novel contrast-induced acute kidney injury model based on the 5/6-nephrectomy rat and nephrotoxicological evaluation of iohexol and iodixanol in vivo, Oxid. Med. Cell. Longev. 2014 (2014), 427560, https://doi.org/10.1155/2014/427560. Epub 2014 Nov 11.

[6] Esther Kneepkens, Edwin Heijman, Jochen Keupp, Steffen Weiss, Klaas Nicolay, Holger Grüll, Interleaved mapping of temperature and longitudinal relaxation rate to monitor drug delivery during magnetic resonance–guided high-intensity focused ultrasound-induced hyperthermia, Invest. Radiol. 52 (10) (2017) 620–630, https://doi.org/10.1097/RLI.0000000000000392.

[7] H. Sakai, K. Sou, H. Horinouchi, K. Kobayashi, E. Tsuchida, Haemoglobin-vesicles as artificial oxygen carriers: present situation and future visions, J. Intern. Med. 263 (1) (2008) 4–15, https://doi.org/10.1111/j.1365-2796.2007.01893.x.

[8] Amir Abbas Momtazi-Borojeni, Mahmoud R. Jaafari, Maciej Banach, Armita Mahdavi Gorabi, Hedayat Sahraei, A. Amirhossein Sahebkar, Pre-clinical evaluation of the nanoliposomal antiPCSK9 vaccine in healthy non-human primates, Vaccines (Basel) 9 (7) (2021) 749, https://doi.org/10.3390/vaccines9070749.

[9] Hiromi Sakai, Yohei Masada, Hirohisa Horinouchi, Eiji Ikeda, Keitaro Sou, Shinji Takeoka, Makoto Suematsu, Masuhiko Takaori, Koichi Kobayashi, Eishun Tsuchida, Physiological capacity of the reticuloendothelial system for the degradation of hemoglobin vesicles (artificial oxygen carriers) after massive intravenous doses by daily repeated infusions for 14 days, J. Pharmacol. Exp. Therapeut. 311 (3) (2004) 874–884, https://doi.org/10.1124/jpet.104.073049. Epub 2004 Aug 5.

[10] Kazuaki Taguchi, Yukino Urata, Makoto Anraku, Toru Maruyama, Hiroshi Watanabe, Hiromi Sakai, Hirohisa Horinouchi, Koichi Kobayashi, Eishun Tsuchida, Toshiya Kai, Masaki Otagiri, Pharmacokinetic study of enclosed hemoglobin and outer lipid component after the administration of hemoglobin vesicles as an artificial oxygen carrier, Drug Metab. Dispos. 37 (7) (2009) 1456–1463, https://doi.org/10.1124/dmd.109.027094. Epub 2009 Apr 13.

[11] Hao Xu, Tymish Y. Ohulchanskyy, Artem Yakovliev, Zinyuk Roman, Jun Song, Liwei Liu, Junle Qu, Zhen Yuan, Nanoliposomes Co-encapsulating CT imaging contrast agent and photosensitizer for enhanced, imaging guided photodynamic therapy of cancer, Theranostics 9 (5) (2019) 1323–1335, https://doi.org/10.7150/thno.31079.eCollection2019.

[12] Srinivasan Mukundan Jr., Ketan B. Ghaghada, Cristian T. Badea, Chen-Yu Kao, Laurence W. Hedlund, James M. Provenzale, G Allan Johnson, Emmanuel Chen, Ravi V. Bellamkonda, Ananth Annapragada, A liposomal nanoscale contrast agent for preclinical CT in mice, AJR Am. J. Roentgenol. 186 (2) (2006) 300–307, https://doi.org/10.2214/AJR.05.0523.

[13] T. Kure, H. Sakai, Transmembrane difference in colloid osmotic pressure affects the lipid membrane fluidity of liposomes encapsulating a concentrated protein solution, Langmuir 33 (6) (2017) 1533–1540, https://doi.org/10.1021/acs.langmuir.6b04643. Epub 2017 Jan 31.

[14] T. Kure, H. Sakai, Preparation of artificial red blood cells (hemoglobin vesicles) using the rotation-revolution mixer for high encapsulation efficiency, ACS Biomater. Sci. Eng. 7 (2021) 2835–2844, https://doi.org/10.1021/acsbiomaterials.1c00424. Epub 2021 May 24.

[15] G. Niu, Experimental histopathological studies of renal lesions induced by high- or low-osmolality contrast media [article in Japanese], Nihon Ika Daigaku Zasshi 60 (6) (1993) 390–405, https://doi.org/10.1272/jnms1923.60.390.

[16] Hiromi Sakai, Kenichi Tomiyama, Yohei Masada, Shinji Takeoka, Hirohisa Horinouchi, Koichi Kobayashi, Eishun Tsuchida, Pretreatment of serum containing hemoglobin vesicles (oxygen carriers) to prevent their interference in laboratory tests, Clin. Chem. Lab. Med. 41 (2) (2003) 222–231, https://doi.org/10.1515/CCLM.2003.036.

[17] K. Sou, R. Komine, H. Sakai, Clinical laboratory test of blood specimens containing hemoglobin-vesicles –interference avoidance by addition of dextran, Artifical blood 17 (1) (2009) 6–15.

[18] Jinzi Zheng, Gregory Perkins, Kirilova Anna, Christine Allen, David A. Jaffray, Multimodal contrast agent for combined computed tomography and magnetic

resonance imaging applications, Invest. Radiol. 41 (3) (2006) 339–348, https://doi.org/10.1097/01.rli.0000186568.50265.64.
[19] Mariska de Smet, Nicole M. Hijnen, Sander Langereis, Aaldert Elevelt, Edwin Heijman, Ludwig Dubois, Philippe Lambin, Holger Grüll, Magnetic resonance guided high-intensity focused ultrasound mediated hyperthermia improves the intratumoral distribution of temperature-sensitive liposomal doxorubicin, Invest. Radiol. 48 (6) (2013) 395–405, https://doi.org/10.1097/RLI.0b013e3182806940.
[20] Esther Kneepkens, Adriana Fernandes, Klaas Nicolay, Holger Grüll, Iron(III)-Based magnetic resonance–imageable liposomal T1 contrast agent for monitoring temperature-induced image-guided drug delivery, Invest. Radiol. 51 (11) (2016) 735–745, https://doi.org/10.1097/RLI.0000000000000297.
[21] Michael Peller, Alenka Schwerdt, Hossann Martin, Herbert M. Reinl, Tungte Wang, Steven Sourbron, Manfred Ogris, Lars H. Lindner, MR characterization of mild hyperthermia-induced gadodiamide release from thermosensitive liposomes in solid tumors, Invest. Radiol. 43 (12) (2008) 877–892, https://doi.org/10.1097/RLI.0b013e31818768cd.
[22] Xavier Montet, Catherine M. Pastor, Jean-Paul Vallée, Christoph D. Becker, Geissbuhler Antoine, Denis R. Morel, Paolo Meda, Improved visualization of vessels and hepatic tumors by micro-computed tomography (CT) using iodinated liposomes, Invest. Radiol. 42 (9) (2007) 652–658, https://doi.org/10.1097/RLI.0b013e31805f445b.
[23] Ehsan Samei, Robert S. Saunders, Cristian T. Badea, Ketan B. Ghaghada, Laurence W. Hedlund, Yi Qi, Hong Yuan, Rex C. Bentley, Srinivasan Mukundan Jr., Micro-CT imaging of breast tumors in rodents using a liposomal, nanoparticle contrast agent, Int. J. Nanomed. 4 (2009) 277–282.
[24] Cristian T. Badea, Khannan K. Athreya, Gabriela Espinosa, Darin Clark, A Paiman Ghafoori, Yifan Li, David G. Kirsch, G Allan Johnson, Ananth Annapragada, Ketan B. Ghaghada, Computed tomography imaging of primary lung cancer in mice using a liposomal-iodinated contrast agent, PLoS One 7 (4) (2012), e34496, https://doi.org/10.1371/journal.pone.0034496. Epub 2012 Apr 2.
[25] Ketan B. Ghaghada, Amy F. Sato, Zbigniew A. Starosolski, John Berg, David M. Vail, Computed tomography imaging of solid tumors using a liposomal-iodine contrast agent in companion dogs with naturally occurring cancer, PLoS One 11 (3) (2016 31), e0152718, https://doi.org/10.1371/journal.pone.0152718.eCollection2016.
[26] C.B. Johansen, A.C. T Martinsen, T.R. Enden, M. Svanteson, The potential of iodinated contrast reduction in dual-energy CT thoracic angiography; an evaluation of image quality, Radiography 28 (1) (2022 Feb) 2–7, https://doi.org/10.1016/j.radi.2021.07.006. Epub 2021 Jul 21.
[27] N. Kiss, P. Hamar, Histopathological evaluation of contrast-induced acute kidney injury rodent models, BioMed Res. Int. 2016 (2016), 3763250, https://doi.org/10.1155/2016/3763250. Epub 2016 Nov 16.
[28] A. Fukatsu, Zoueizai, in: T. Yasuda, N. Hirawa, Y. Oyama (Eds.), Clinigal Nephrology, first ed., Nanzando, Tokyo, 2013, pp. 704–709.
[29] S.N. Heyman, C. Rosenberger, S. Rosen, Regional alterations in renal haemodynamics and oxygenation: a role in contrast medium-induced nephropathy, Nephrol. Dial. Transplant. 20 (Suppl 1) (2005) i6–i11, https://doi.org/10.1093/ndt/gfh1069.
[30] Sachse A. Iodinated liposomes as contrast agents. In: Blute JW, Modo M eds. Nanoparticles in Biomedical Imaging. New York: Springer Science+Business Media. pp 371-410.
[31] Satoshi Yasumura, Masanori Matsumoto, Shigemi Makino, Shuichi Kino, Asashi Tanaka, Takehiro Kohno, Akito Nozaki, Koji Matsuzaki, Yuji Yonemura, Tadashi Matsushita, Evidence-based guidelines for the use of albumin products, Second Edition, Japanese Journal of Transfusion and Cell Therapy 64 (6) (2018) 700–717.
[32] Chatchai Kreepala, Atitaya Srila-On, Maethaphan Kitporntheranunt, Watcharapong Anakkamatee, Popthum Lawtongkum, Krittanont Wattanavaekin, The association between GFR evaluated by serum cystatin C and proteinuria during pregnancy, Kidney Int Rep 4 (6) (2019) 854–863, https://doi.org/10.1016/j.ekir.2019.04.004.eCollection2019Jun.
[33] H. Sakai, H. Horinouchi, K. Tomiyama, E. Ikeda, S. Takeoka, K. Kobayashi, E. Tsuchida, Hemoglobin-vesicles as oxygen carriers: influence on phagocytic activity and histopathological changes in reticuloendothelial system, Am. J. Pathol. 159 (3) (2001) 1079–1088, https://doi.org/10.1016/S0002-9440(10)61783-X.